



Gummel-Poon modeling of a New Super-Gain BJT and an innovative 600V AC switch

Zheng Ren, Nathalie Batut, Ambroise Schellmanns

► To cite this version:

Zheng Ren, Nathalie Batut, Ambroise Schellmanns. Gummel-Poon modeling of a New Super-Gain BJT and an innovative 600V AC switch. Symposium de Genie Electrique, Jun 2016, Grenoble, France. <hal-01361544>

HAL Id: hal-01361544

<https://hal.archives-ouvertes.fr/hal-01361544>

Submitted on 7 Sep 2016

HAL is a multi-disciplinary open access archive for the deposit and dissemination of scientific research documents, whether they are published or not. The documents may come from teaching and research institutions in France or abroad, or from public or private research centers.

L'archive ouverte pluridisciplinaire **HAL**, est destinée au dépôt et à la diffusion de documents scientifiques de niveau recherche, publiés ou non, émanant des établissements d'enseignement et de recherche français ou étrangers, des laboratoires publics ou privés.

Gummel-Poon modeling of a New Super-Gain BJT and an innovative 600V AC switch

Zheng REN¹, Pangen WANG², Ambroise SCHELLMANN^{1,2}, Nathalie BATUT^{1,2}, Yoann BUVAT³

¹ GREMAN UMR-CNRS 7347, 7 avenue Marcel Dassault, 37200 Tours, France

² Electronics and Energy Department, Polytech'Tours, University of Tours, France

³ R&D Department, STMicroelectronics, Tours, 37100, France

Email: zheng.ren@univ-tours.fr

Abstract – This paper deals with the static electrical modeling of the super-gain BJT and the innovative 600V AC switch solution which it gives to. As power bipolar component, their modeling is based on the Gummel-Poon model which is widely accepted and used by researchers as well as circuit simulators like Pspice. All of the model parameters are extracted from device characterization data via extraction mathematical equations. The modeling of the super-gain BJT is mainly composed of two separate parts which is respectively the forward-biased modeling and the reverse-biased modeling. The characterization test bench is presented, than the extraction methods of respective parameter category are also introduced in this paper as well as the data processing method. The validation of the extracted model parameters will be done by comparing the SPICE simulation results with experimental ones under the same condition. The comparison result proves a good coherence between simulations and experimentations.

Key Words — Modeling, super-gain BJT, AC switch, Gummel-Poon, Characterization, parameter extraction.

1. INTRODUCTION

In the development of modern power electronics, new power switch has always been a priority and “hot spot” for both industries and researchers. The applications such as intelligent grid and smart buildings require the replacement of conventional mechanical and electromechanical switches by innovative performing power electronic devices [1], [2]. In this context, the GREMAN laboratory has designed and manufactured a super-gain ($h_{FE} > 220$) Gate Associated Bipolar Junction Transistor. In order to fully explore the potential of this device, an innovative 600V AC switch solution has been proposed, named as “TBBS” (Transistor Based Bidirectional Switch). The concept of the super-gain BJT and its physical structure are presented in **Fig.1**. The thin ($1.5\mu\text{m}$) and lightly doped ($[Dop_B] > 1.10^{16} \text{at.cm}^{-3}$) Base makes the DC current gain of super-gain BJT very important in both forward-biased mode (h_{FE}) and reverse-biased mode (h_{FC}) [3]. This result gives birth to our innovative 600V AC switch which is named TBBS, short for Transistor Based Bidirectional Switch. The TBBS is composed of two super-gain BJTs in anti-serial [4], as is shown in **Fig.2**. The static mode characterization of the super-gain BJT and the TBBS, which shows us their promising and encouraging electrical characteristics on controllability and conduction power dissipation, has been described in [5].

In order to be able to integrate this new AC switch into applications and to better understand the impact of its physical structure on its electrical behavior, a reliable and robust SPICE model should be created and this must pass through the electrical modeling for an elementary super-gain BJT. So in the first part of this paper, the electrical modeling method of the super-gain BJT is introduced. The electrical modeling of the TBBS is presented in the second part. Their SPICE simulation results will be presented and discussed for the first time.

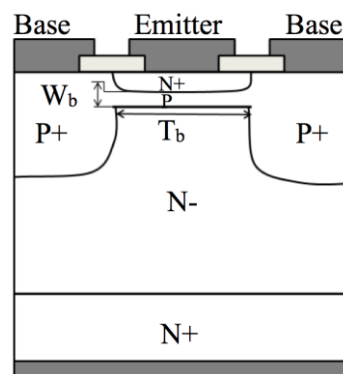


Fig. 1 Cross-sectional view of the super-gain BJT

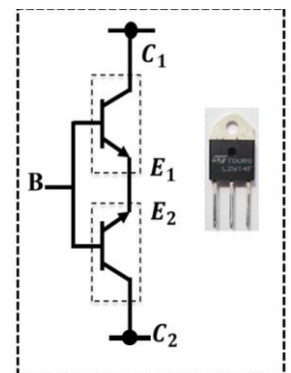


Fig. 2 Representative diagram of TBBS: two super-gain BJTs in anti-serial

Table. 1 Comparison on conduction power dissipation of existing AC switch solutions

AC switch solutions	On-state power dissipation ($I_c = 1 \text{ A}$, $T_j = 25 \text{ }^\circ\text{C}$)
Thyristor or in antiparallel	1 W/A
TRIAC	1 W/A
Diode bridge + IGBT	2 W/A
IGBTs + Diodes	2 W/A
SJ-MOSFET + Diodes	0.9 W/A
TBBS	0.29 W/A

2. ELECTRICAL MODELING OF THE SUPER-GAIN BJT

The application and further study of the super-gain BJT requires electrical simulations, so a SPICE model of the super-gain BJT should be established. Thus the widely used SPICE model Gummel-Poon has been chosen for its modeling. This model was initially proposed by Hermann Gummel and H. C. Poon in 1970s in order to simulate the working principal of the bipolar transistor. The Gummel-Poon model takes the physical operation mechanism of the BJT into consideration, so it can give us a good description on the static and dynamic electrical behavior of the super-gain BJT. The Gummel-Poon large signal schematic of the bipolar transistor is shown as **Fig.3**.

The two PN junctions of the BJT are replaced by inner diodes and the phenomenon of the depletion capacitance of the junction is presented by external capacitors such as $C_{B'C'}$ and $C_{B'E'}$. The parasitic resistances of the bonding and packaging, which can have a huge impact on its electrical performance under high injection, are modeled by external resistances such as R_C and R_E .

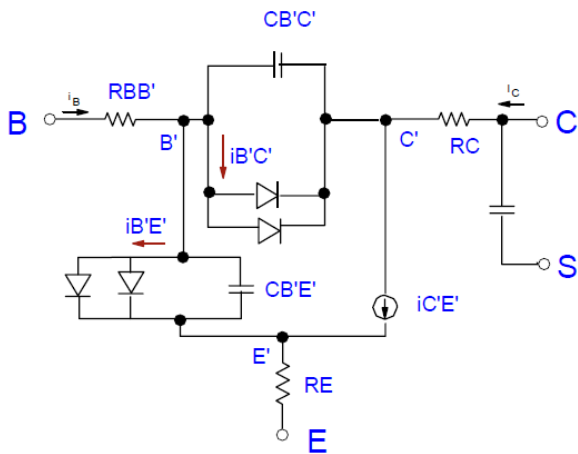


Fig. 3 Large signal schematic of the BJT (Gummel-Poon model)

The electrical modeling procedure including electrical characterization and model parameter extraction is mainly based on the method described in [6]. There are over 30 parameters implemented in Gummel-Poon model and they are divided into four categories: capacitance parameters, resistance parameters, DC parameters and transient parameters. The parameter extraction procedure follows the same order as the increase dependence of respective step with the former ones.

2.1. DC electrical characterization

The establishment of the DC electrical modeling and the parameter extraction procedure require several types of characterization data. For example the extraction of the capacitance parameters needs the C-V measurement of the Base-Emitter junction and the Base-Collector junction. The determination of the forward-biased Early voltage effect requires the output characteristics (I_C - V_{CE}) for different level of the base current. And the high current roll-off parameter (I_{KR} and I_{KF}) needs to be extracted from the forward-biased and reverse-biased Gummel plot.

The characterization bench has been set up according to the diverse measurement requirement described above, it will be introduced in this part along with some important characterization results. It has to remark that, in order to minimize the parasitic capacitance of packaging and the parasitic resistance of bonding, all of the electrical characterizations for parameter extraction have been done on wafer with probing tester under controlled temperature (300K) at the CERTEM platform of GREMAN laboratory.

2.1.1. Characterization bench

The characterization bench is presented as **Fig.4**. It is composed of several characterization equipment.

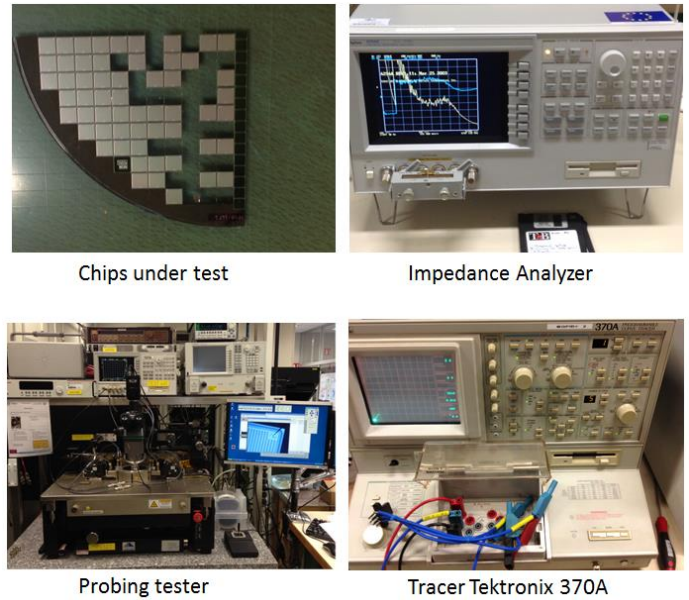


Fig. 4 Characterization bench and components under test

Probing tester allows us to access to the different contacts of a single chip, it is the intermediate between the under test chips and other characterization equipment. It has to remark that this kind of probing tester station is designed to measure components on wafer, but for the measurement of isolated silicon chips, a reliable fixture should be implemented and the contact between the contacts and the probes should be manipulated carefully to prevent any potential surface damage to the chips. A surface check under microscope is strongly recommended after contacting the probes.

Impedance analyzer Ailgent 4294A performs the C-V measurement (Capacitance versus Voltage) of every junction for capacitance parameter extraction. Tracer Tektronix 370A is used here to obtain DC curves under different test conditions for DC parameter extractions. Particularly, the Kellog network (I_C versus V_{CE} for different I_B) and the Gummel plot of the super-gain BJT in both forward-biased and reverse-biased should be obtained. And the previous work of our study shows that the forward-biased and reverse-biased quasi-saturation voltage are about 0.3V, so the Gummel plot will be traced under this voltage.

2.1.2. Characterization results

Some of the critical characterization results will be presented in this part, including resistance measurement, capacitance measurement and DC characterization curves.

The extraction of the ohmic parameters requires the evolution of every parasitic resistance (Base resistance R_B , Base resistance at high injection R_{BM} , Emitter resistance R_E and Collector resistance R_C) versus Base current. We take the Emitter resistance R_E as an example to present the extraction procedure and result. The “fly-back” method is used in our characterization. A Base current is applied and the Emitter pin is grounded, we measure the voltage which is proportional to the Base current at the open Collector. If we derivate V_{CE} with respect to I_B , we get the equivalent R_E for each operating point. The value of R_E is then the mean value of the flat range in this plot. The obtained curve for R_E is presented as Fig.5.

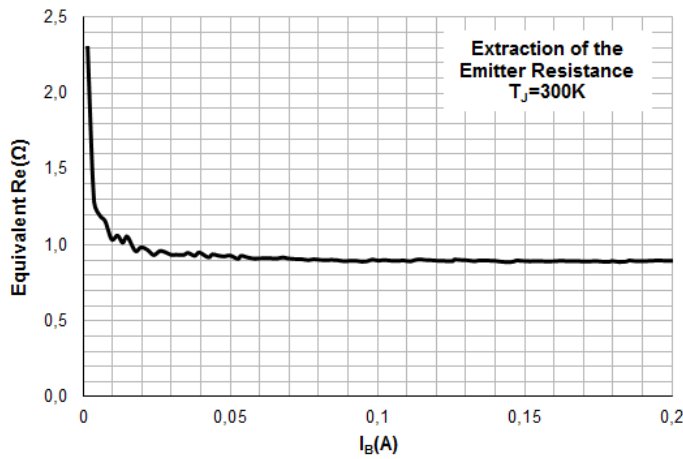


Fig. 5 Characterization result of the Emitter Resistance, R_E versus I_B when the junction temperature (T_j) is 300K

The extraction of the capacitance parameters requires the C-V measurement of every junction. For the measurement of the Base-Emitter capacitance, the Collector is left open while the Emitter is open during the measurement of the Base-Collector capacitance. In both cases, the modeling formula is identical, so only the C-V measurement result of the Base-Emitter is presented here in Fig.6.

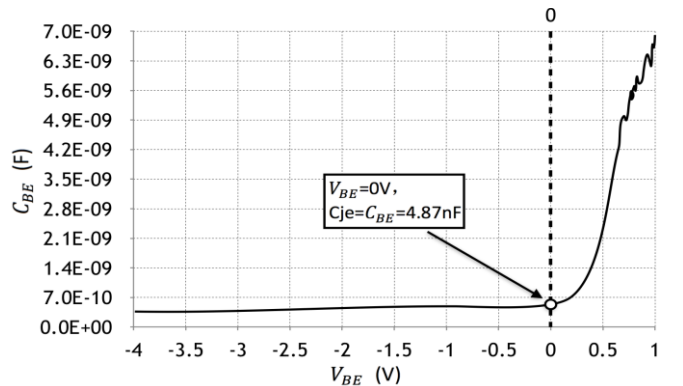


Fig. 6 Characterization result of the space charge capacitor: C-V measurement of the Base-Emitter junction

As the super-gain BJT is designed as a power switch, so its Gummel plot in quasi-saturation region is very important for the accurate electrical modeling. The forward-biased Gummel plot is presented in Fig.7. The pre-defined quasi-saturation voltage is 0.3V according to the static mode characterization [1]. It has to mark that the junction temperature can have a significant influence on the Gummel-Plot, so junction temperature should be regulated when the collector current is larger than 10mA.

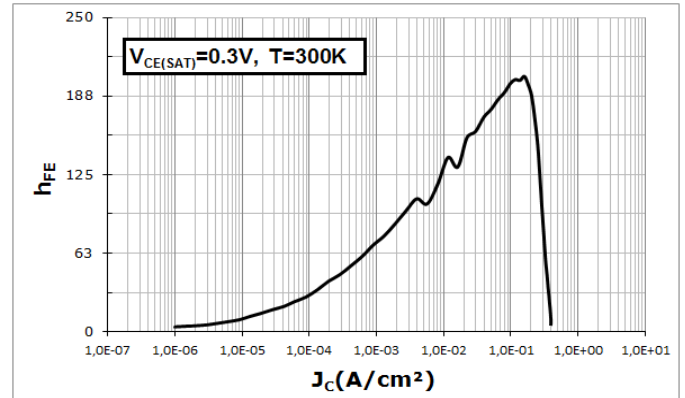


Fig. 7 Characterization result of the forward-biased Gummel plot. Quasi-saturation voltage $V_{CE(SAT)}$ is 0.3V and the junction temperature is controlled to 300K.

In order to quantify the effect of the Base Width Narrowing, the forward and reverse Early voltage of the super-gain BJT should be measured. The Kellogg network can be used here to extract the Early voltage, one of the obtained Kellogg network is presented as Fig.8.

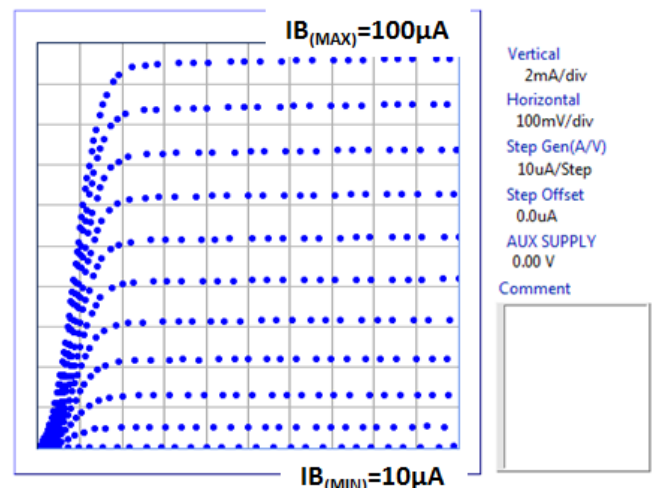


Fig. 8 Kellogg network (Collector current I_C versus Collector voltage V_{CE} under different Base current I_B)

The obtained Gummel plot as well as Kellogg network allow us to extract many nonlinear DC parameters, especially the ones who can play an important role in low level Collector current density.

2.2. Data processing and parameter extraction

The data processing and parameter extraction can be mainly divided into 4 parts: capacitance parameters, resistance parameters, DC parameters and transient parameters. The same extraction order is followed because the increase dependence between every set of parameter with its former one, which means the capacitance parameters have the lowest influence on the others parameters of the model, but on the contrary, the DC parameters have great dependence with the capacitance and resistance parameters. We follow the same order to present our extraction method and we take one representative parameter from each group as example.

2.2.1. Capacitance parameter extraction

The capacitance parameter extraction should be done respectively for the two junctions of the super-gain BJT, here the parameter extraction procedure for Base-Emitter is presented as an example.

The behavior of the space charge capacitor is given by equation (1):

$$C_{SBE} = \frac{C_{JE}}{(1 - F_C)^{(1+M_{JE})}} * \left[1 - F_C * (1 + M_{JE}) + M_{JE} * \frac{v_{BE}}{V_{JE}} \right]$$

- C_{JE} : Base-Emitter zero bias depletion capacitance
- V_{JE} : Base-Emitter Built-in potential
- M_{JE} : Base-Emitter junction exponential factor
- F_C : Forward bias depletion capacitance coefficient

The value of the C_{JE} can be obtained directly from the C-V measurement curve, it is the space charge capacitor when the bias of the junction is 0V. The F_C is a constant coefficient of 0.5. Along with the measured point (C_{SBE} , V_{BE}), the rest of the parameter can be extracted from the linear regression of the positive linear part of the C-V measurement curve.

It has to notice that the measurement of the junction space capacitor is very sensible to external influences. So in order to minimize the parasitic capacitor introduced by equipment, the average value for several examples is strongly recommended. Here we take the average value of 3 super-gain BJTs. The extracted capacitance parameters of the Base-Emitter junction are presented as following:

$$M_{JE}=0.53 \quad C_{JE}=4.92\text{nF} \quad V_{JE}=0.6\text{V}$$

2.2.2. Nonlinear DC parameters extraction

It has to remark that the measured data should be carefully selected for DC parameter extraction. The improper choice could easily lead to unreasonable value or even to one of the famous, so called "infinite modeling loops".

For example the extraction of Base-Emitter leakage emission coefficient (N_E) should be done with low V_{BE} data and the Forward beta hi current roll-off (I_{KF}) should be extracted under high current. The wrong choice of data range could lead to unreasonable parameter value. Another important extraction technique is the application of the 'Loss function'. This function reflects the error between estimated and true value for an instance of data, seeking for the minimized error

could help the parameter estimation. The extraction of I_{KF} is taken here as an example of this technique.

I_{KF} is extracted from the equation (2):

$$E = \sum_{i=1}^N \left\{ \frac{I_{Bi}}{I_{Ci}} \times \frac{1 - \frac{I_{Ci}}{I_{KF}} - \frac{V_{BCi}}{V_{AF}} - \frac{V_{BC}}{V_{AR}}}{\frac{1}{B_F} + \frac{I_{SE}}{I_S} \times \exp\left\{\frac{V_{BEi}}{V_T} \left[\frac{1}{N_E} - \frac{1}{N_F}\right]\right\}} \right\}^2 \quad (2)$$

Here in this equation, 'E' stands for total error and it is the loss function which has I_{KF} as its only variable. This function is solved for a best I_{KF} by iteration. The evolution of the total error in terms of I_{KF} is demonstrated as **Fig.9**. As shown in the figure above, the I_{KF} is determined when the total error is minimized. Many other model parameters are extracted by using the same technique.

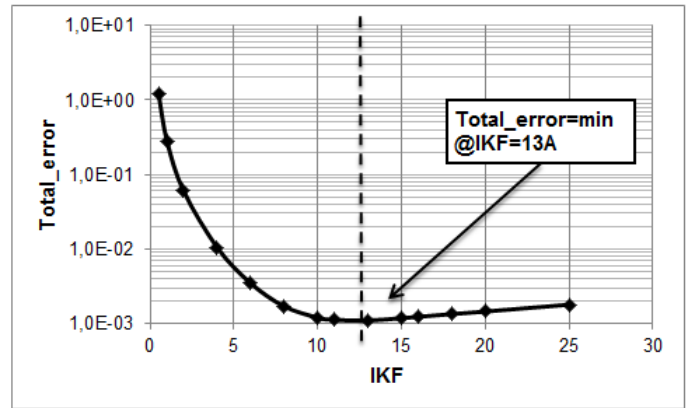


Fig. 9 Extraction of $I_{KF}=13\text{A}$, when the Total_error of the loss function are minimized

2.3. Results and conclusions of the super-gain BJT

After completing the model parameter extraction procedure, the reliability and robustness of the extracted parameters are verified by comparing the simulation results of the established model with the experimental ones. Keep in mind that the complete modeling is carried on for both forward-biased mode and reverse-biased mode, so the modeling result will be presented for these two aspects. More precisely, for each polarization, the output curve and the Gummel plot of the super-gain BJT are traced and compared with measured ones.

2.3.1. Modeling result in forward-biased mode

The forward-biased modeling result is introduced by presenting its output curve (**Fig.10**) and its Gummel plot (**Fig.11**). They are also compared with correspond experimental curves. The output curve represents the I-V characteristics of the super-gain BJT for a fixed current of Base. The Gummel plot reflects its amplification performance in a large range of I_B for a specific Collector-Emitter voltage. They are two dimensions to evaluate the performance of a BJT. Here we choose the V_{CE} voltage at 0.3V because the quasi-saturation region of the super-gain BJT is found nearby this region.

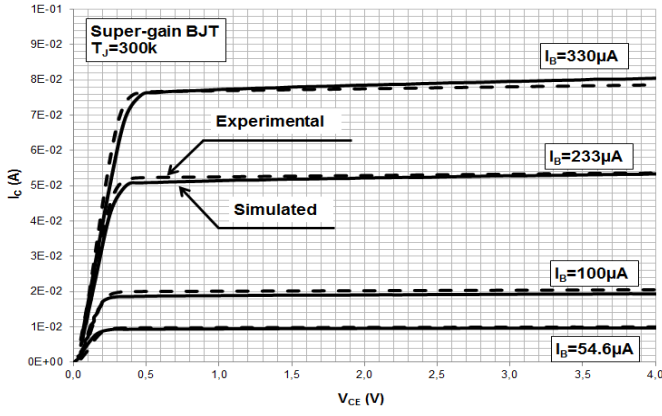


Fig. 10 Comparison of the forward-biased simulated output curve and the experimental curve under different base current level and controlled junction operating temperature (300K)

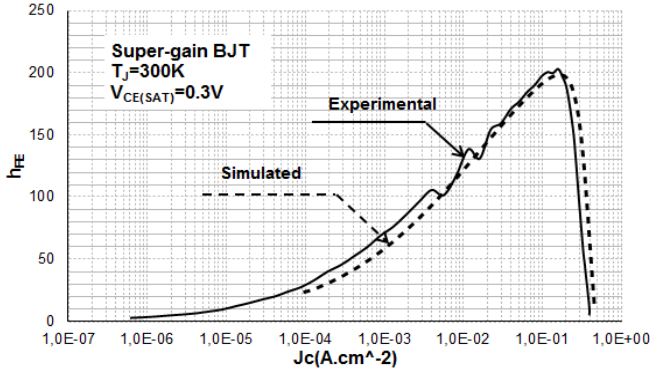


Fig. 11 Comparison of the forward-biased simulated Gummel curve and the experimental curve under the same Collector-Emitter saturation voltage $V_{CE(SAT)}=0.3V$ and operating temperature (300K)

In order to quantify the difference between the simulated and experimental curve, the absolute error is introduced. The absolute error is calculated according to the equation (3):

$$E_{abs} = \frac{1}{n} \sqrt{\sum_{i=1}^n \left(\frac{y_{mes} - \hat{y}_{sim}}{y_{mes}} \right)^2} \quad (3)$$

- E_{abs} : Absolute error between simulation and measurement curves
- y_{mes} : Measurement value
- \hat{y}_{sim} : Simulation value

The absolute error of the forward-biased output curve is **4%** and that of the Gummel plot is **8.1%**. This result is pretty satisfactory as the two absolute errors are all below 10%.

2.3.2. Modeling result in reverse-biased mode

Considering the symmetrical structure of the bipolar junction transistor, the reverse Gummel-Poon parameters are extracted in nearly the same way regarding to the forward ones. The only difference is to exchange the Collector and Emitter for characterization and extraction equations. The reverse-biased modeling result is presented in the same way in **Fig.9** and **Fig.10**.

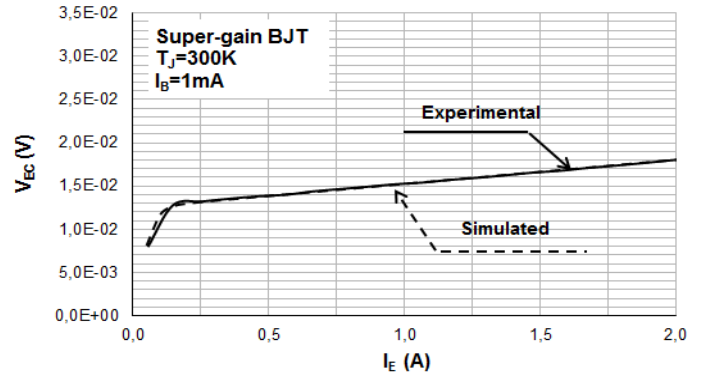


Fig. 12 Comparison of the reverse-biased simulated output curve and the experimental curve under the same base current level (1mA) and operating temperature (300K)

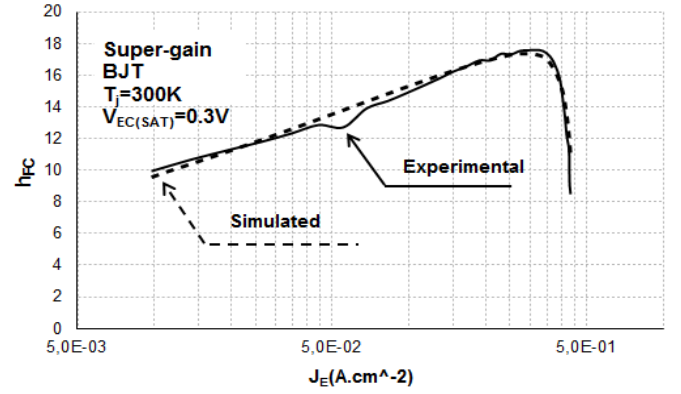


Fig. 13 Comparison of the reverse-biased simulated Gummel curve and the experimental curve under the same Emitter-Collector saturation voltage $V_{EC(SAT)}=0.3V$ and operating temperature (300K)

The absolute error of the reverse-biased output curve and Gummel plot is respectively **1.2%** and **2%**. Small absolute errors in both forward and reverse-biased mode prove a good coherence between obtained electrical model and the real component, which also confirm the reliability of our electrical characterization and parameter extraction procedure. The Gummel-Poon model of the super-gain BJT has been established and this will conduct us to the modeling of the 600V AC switch TBBS.

3. ELECTRICAL MODELING OF THE TBBS

After the static electrical modeling of one single super-gain BJT, we are now interested in the modeling of the AC switch TBBS. As mentioned in the introduction, the TBBS is composed with two super-gain BJTs connected in anti-serial. More precisely, the two Emitters will be connected and the two Bases will be shorted. So the Collectors of the two elementary super-gain BJT will become the power dies of the AC switch which are named respectively as C1 and C2.

It has to remark that the prototype of the TBBS has been done by assembling two discrete super-gain BJTs on one adaptor. And the junction temperature is regulated by dielectrical oil bath during the characterization. The successful

modeling of the TBBS cannot be achieved by simply connecting two super-gain BJT electrical model in anti-serial. The equivalent parasitic resistance R_E and R_C are much smaller for the TBBS. So additional resistances R_{EP} and R_{CP} are introduced into its modeling in parallel with Collector and Emitter parasitic resistance, as is shown in Fig.13.

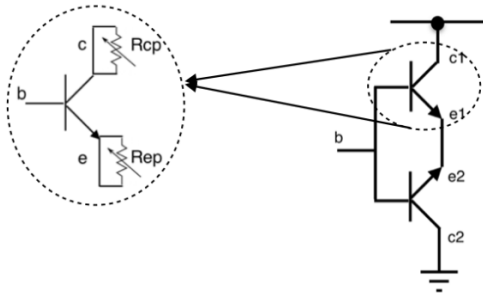


Fig. 14 Representative diagram of the additional parallel resistance for the modeling of the TBBS

Many iterative simulations have been carried on to determine the optimal value of R_{EP} and R_{CP} . Here we choose the Gummel Plot accuracy as criteria to locate their optimal value. The best Gummel Plot accuracy can be found when the R_{EP} is 0.075Ω and R_{CP} is 0.166Ω . The comparisons between simulation result and measured result are presented in Fig.15 and Fig.16.

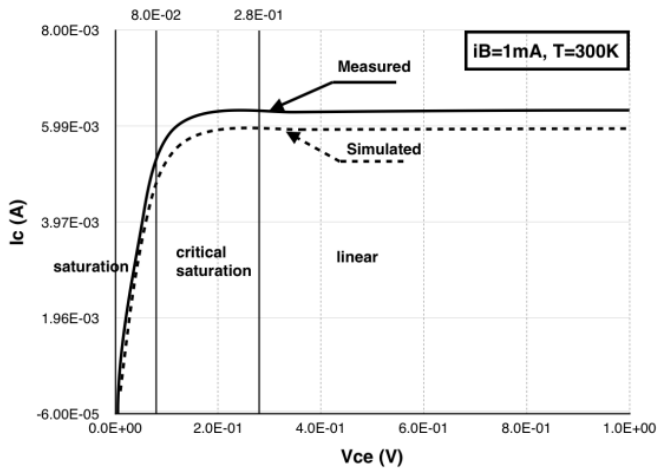


Fig. 15 Comparison of the simulated output curve and the experimental curve of TBBS under the same base current level (1mA) and operating temperature (300K)

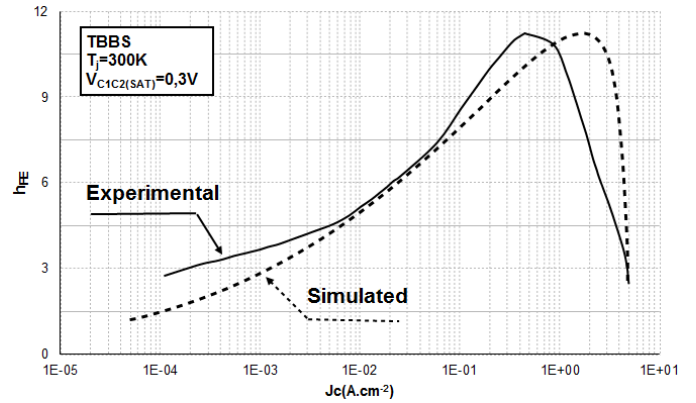


Fig. 16 Comparison of the simulated Gummel curve and the experimental curve of the TBBS under the same Emitter-Collector saturation voltage $V_{C1C2(SAT)}=0.3V$ and operating temperature (300K)

The absolute error between the simulated and experimental output curve is 9.8% and that of the Gummel curve is 7.9%. Because of the symmetrical structure of the TBBS, the reverse-biased simulation and experimentation results will be the same as that of the forward-bias.

4. CONCLUSIONS AND DISCUSSION

The static electrical SPICE model of the super-gain BJT and the TBBS have been established. The Gummel-Poon BJT model is used in the modeling and all of the model parameters are extracted from physical measurement followed by the mathematical extraction method. The comparison between simulated and experimental output curve and Gummel plot shows us a good accuracy of their model. The absolute error of every simulated curve comparing to their measured ones are always less than 10%. The establishment of their SPICE model allows us to better explore the functionality of TBBS and to integrate it in a dedicated application such as domestic photovoltaic inverter.

5. REFERENCES

- [1] A. Amerasekera, Ultra low power electronics in the next decade, Proceedings of the IEEE International Symposium on Low-Power Electronics and Design, 2010, p. 237.
- [2] G. Anastasi, F. Corucci, F. Marcelloni, An intelligent system for electrical energy management in buildings, Proceedings of the International Conference on Intelligent Systems Design and Applications, 2011, pp. 702-707.
- [3] L.-V. Phung et al, Modeling of a new SOI bidirectional bipolar junction transistor for low-loss household appliances, IEEE Transactions on Electron Devices, Vol. 58, No 4, 2011, pp. 1164-1169.
- [4] Batut.N et al., "Development and Characterization of a New Low-loss Monolithic AC Switch", Proceedings of the 26th International Symposium on Power Semiconductor Devices & ICs (ISPSD'2014), Hawaii, USA, June 2014. E. P. Wigner, "Theory of traveling-wave optical laser," Phys. Rev., vol. 134, pp. A635-A646, Dec. 1965.
- [5] Zheng. REN et al., "Development and Static Mode Characterization of a New Low-loss AC Switch Based on Super-Gain BJT", Special issue published in Journal of Energy and Power Engineering in January 2014.
- [6] Franz Sischka, "Gummel-Poon Bipolar Model, model description and parameter extraction", Agilent Technologies GmbH, 2006, Munich (Germany)